POAC'17
Busan, KOREA

Proceedings of the 24th International Conference on
Port and Ocean Engineering under Arctic Conditions
June 11-16, 2017, Busan, Korea

Confederation Bridge - Lessons and What They Tell Us about the Flexural Failure of Ice

Thomas G Brown[1], Noorma Shrestha[1]
[1] University of Calgary, Calgary, Canada

ABSTRACT

Monitoring systems for the measurement of ice forces and the observation of attendant ice conditions have been in place on several piers of Confederation Bridge, since it opened in 1997. The resulting database of ice interactions is very extensive, amounting to some 20,000 discrete interaction events, many of which have been analyzed in detail. The paper provides a detailed summary of the findings from this monitoring program. These relate to the characteristics of the interaction between ice and the conical piers, the relationship between these characteristics and the resulting ice force, and the relationship between the ice force and the ice physical properties. Because the piers are conical, the ice behavior is flexural. The paper describes the mechanics of the observed ice interactions and how these align and differ from those assumed in accepted ice force algorithms. The paper provides suggestions for improvements to these algorithms, particularly in the treatment of rubble piles and ride-up ice.

KEY WORDS: ice load, flexural failure, ice-conical structure interaction, ice rubble pile.

INTRODUCTION

The monitoring programme at the Confederation Bridge was initiated as a result of uncertainty as to the ice forces on the piers, and the need to understand the behavior of the ice as it interacts with the piers and the forces that result from these interactions. After 18 years of continuous monitoring of ice forces and ice behavior on the two of the main piers of the Confederation Bridge, an extensive ice action database has been created that has provided new insight in flexural failure of ice on conical structures. While the primary emphasis of the monitoring programme has been on the measurement of ice forces, much additional effort has been placed on the measurement of related data and the observation of the behavior of the ice interacting with the piers. These observations includes the behavior of the ice against ice-breaking cones, extracting geometric characteristic of the ice interacting with the piers from ice video, the velocity of the interacting ice, measuring of the pressure and local load distribution resulting from the ice interacting with the pier elements. This paper aims to summarize the findings from the long-term monitoring programme and establish the relationship between ice action and ice physical properties in terms of flexural failure of ice.

ICE LOAD MEASUREMENT

The global ice loads at the Confederation Bridge piers are determined by applying a transfer function from the measured tilts of the pier shaft. The tilts are also corrected for wind effects and baseline shift, detailed in Brown (2007a and 2007b). The tilts at the bottom of the shaft (G3TMY and STMY) are less affected by dynamics due to wind effects than the top tilts and thus are used to determine the global ice load. The tiltmeter data are recorded in two data collection modes, average and trigger. The initial assessment of the ice load is obtained from the average tilt data. In the daily ice load record, ice events, i.e. peak ice load within a predetermined time period that is greater than a preset threshold load (currently set at 0.75 MN), are identified. The time duration is defined by the number of time steps to either side of the peak load and has been set to 10 records of the average file, or 5 records to either side of the peak load, i.e. 170 sec duration for P31 and 150 sec for P32. Trigger data are only collected when pier tilts exceed a threshold and are recorded at intervals of 0.034s for P31 and 0.008s for P32. The number of ice events recorded at the Bridge instrumentation varies every year based on winter condition, availability of both wind and tiltmeter data and reliability of the recorded data. For pier P31 the lowest number of events, 181, was recorded in year 2006 and maximum number of events, 2307, in year 2009. For pier P32, the lowest number of events, 243, was also in year 2006 and maximum number, 1070, was recorded in 1999. For all years from 1998 to 2010, regardless of direction of load, a total of 12,220 ice events at pier P31 and 5,795 ice events at pier P32 had been identified from available average tilt data.

The presence of the Confederation Bridge across the Northumberland Strait has affected the ice conditions in the area. The strong tides, both flood and ebb, and driving forces which move the ice back and forth against the multiple piers, result in either the ice breaking or it lodging against the piers. The ice forces on the piers are a function of a number of different variables (Brown et al., 2010) such as ice growth, ice features, mechanical properties of ice, and ice-structure interaction variables such as rubble height, rubble angle, current velocity, wind speed, tide height etc. The ice concentration upstream (west) of the Bridge is greater than the downstream (east) (Brown et al., 1994), which is also confirmed by the number of events recorded by the instrumentation system at the piers. While not all the variables play a significant role in the final ice load determination, they all have some influence on ice load. In the design process, both the limit stress load (load required to fail the ice feature) and the limit force (driving force) were considered. However, the strong current and prevailing wind regime in the Northumberland Strait ensured that the limit force seldom governed.

The ice load measurement programme on the Confederation Bridge has been in place for the past eighteen years, beginning before the bridge opened in May, 1997. The system was put in place with three objectives: to validate the ice load design criteria, to provide information that could be used in the assessment of the maintenance system on the bridge, with particular emphasis on the ice breaking cones, and to provide a test system for the measurement of ice forces on conical structures.

FLEXURAL FAILURE MODELS

Extensive work to predict ice forces on conical-shaped piers was undertaken in Canada in the mid-1960s for a proposed Confederation Bridge linking Prince Edward Island to the mainland of Canada across the Northumberland Strait (Lavoie, 1966). Some of the earliest flexural failure models for ice-structure interaction include Afanas'ev et al. (1971); Bercha and Danys (1975); Edwards and Croasdale (1976); Pearce and Strickland (1979). In these

models, the global ice force is the sum of a breaking term and a ride-up term. The expressions in these models are based on dimensional analysis with coefficients from linear regression or scale experiments. Other early works on flexural failure model include: Ralston (1977) model based on plastic limit analysis of the ice; Croasdale (1980) 2-D model based on the bending of an elastic beam on an elastic foundation. Some of the recent work includes: Määttänen and Hoikkanen's (1990) model which was based on the ice edge crushing effects and ice pile-up on a wedge shaped beam on an elastic foundation; Nevel (1992) model based on the failure of a truncated wedge on an elastic foundation; Croasdale (1994) 3-D model which was specifically modified for the design of the Confederation Bridge to include three-dimensional effects and the presence of a rubble pile; Lau (1999) model for multi-sloped structure with incorporation of rubble pile up loading. The most recent models developed to simulate ice flexural failure on conical structures was completed by Mayne (2007) and Wong (2014). Both Mayne and Wong models have been largely based on full scale ice-structure observations on the Confederation Bridge.

Mayne Model

Mayne developed a flexural failure model based on ice rubble pile behavior observed at the conical piers of the Confederation Bridge. The Mayne model consists of two main components, the breaking load and the load due to the rubble pile. He observed that the profile of the ice rubble pile resting on the cone and ice sheet can be approximated by a bilinear profile. He proposed to use the 2D method of slices to calculate the loads acting on the conical pier and the advancing ice sheet. Mayne focused on the model of the rubble pile formed around the cone. The breaking load of the Mayne model is derived based on the assumption that the ice sheet can be modelled as a semi-infinite beam on an elastic foundation as devised by Hetényi (1946). The model specifically accommodates the difference in deflection of the ice sheet between the apex of the cone and the sides, where no deflection occurs. One consequence of this acknowledgement of the physics of the interaction is that the "circumferential" crack is not circular but elliptic. Observations of this crack, and there are not many due to the presence of the rubble pile, confirm this crack shape. To calculate the breaking load, the rubble pile is treated either as a triangular load or an equivalent point load. A resolution factor was used in converting the 2D horizontal load into a 3D horizontal load based on the assumption that the rubble pile is axisymmetrical around the conical pier.

From the Confederation Bridge Monitoring Program, Mayne observed that due to the complexity of the non-linear profile, the cross-section of a rubble pile at the front end is mostly non-linear, unlike in other flexural failure models where a linear profile is assumed. The dimensions of the bilinear profile (Figure 1) are determined by the following key parameters: upper and lower profile angles (θ_U and θ_L) and horizontal (X_U, X_R) and vertical (Y_R) distances. These key parameters are determined using image analysis software to measure the image pixels and scaling these pixels to the appropriate dimensions. A bilinear rubble pile geometry means two geometric cases are to be considered.

The first geometry case, Case I, is when the bilinear point is above the cone (Figure 1a). The second case is when this point is above the ice sheet (Figure 1b). As the rubble pile profile for a given interaction event, will vary diversely in dimensions and geometry, the calculation of the overall horizontal load for the rubble portion will depend on the geometric case (I or II). The calculation of the total horizontal flexural load due to ice-structure interaction is sum of breaking load and the rubble load.

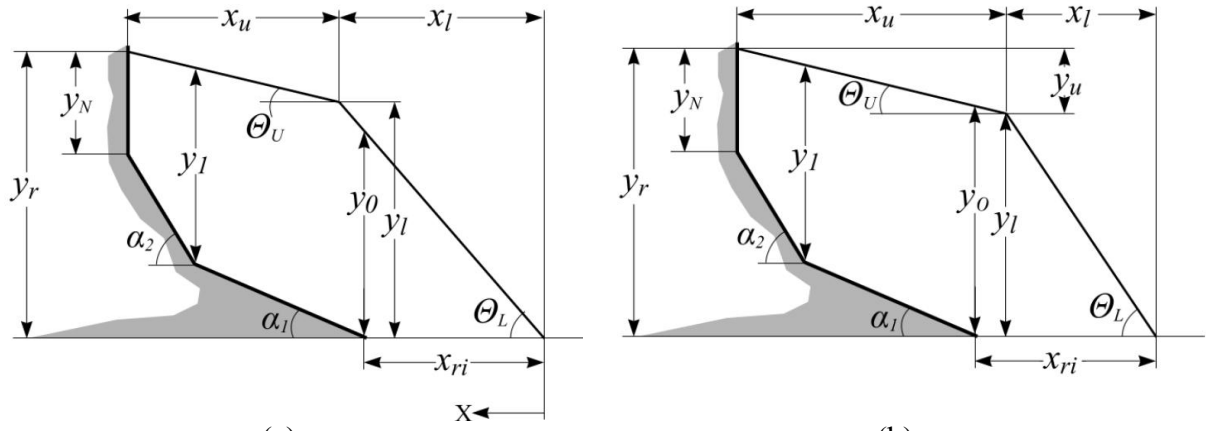

(a) (b)

Figure 1. (a) Case I bilinear rubble profile (b) Case II bilinear rubble profile (Mayne, 2007)

Wong Model

One of main drawback of Mayne model was assuming that the rubble pile is axisymmetrical around the conical pier. The rubble pile geometry from video image analysis only provides the estimated dimensions at the middle cross-section of the ice rubble pile where the maximum height of the pile occurs. To overcome this limitation, Wong (2014) proposed a three-dimensional model for ice rubble interaction on conical structure. Wong modeled the geometry of the ice rubble pile around the conical pier through small-scale tests using a cone, and a pile of gravel. The rubble pile around the cone was divided into ten horizontal strips as shown in Figure 2. It was assumed that each section moves at a same velocity and each section acts independent of adjacent sections. The motion of ice rubble in each section aligns with the direction of the advancing ice sheet and is upward which is in contrast with the assumed direction made in most previous flexural failure models (most models assume that all ice rubbles are pushed up converging toward the pier centre). With the measured rubble pile geometry along ten horizontal strip sections, the rubble load around the cone is estimated by up-scaling results from physical model test (Wong, 2014). The ice rubble loads on the conical pier and ice sheet were determined from a generalized Morgenstern–Price method of slices (Fredlund and Krahn, 1976) to simulate the actual ice rubble pile behavior observed in the field. In Wong model, the slices are aligned parallel to the direction of motion, whereas the slices in the Mayne model are aligned perpendicular to the direction of motion. The behavior includes ice rubble formation, ride-up, and motion. A 3D finite element program was used to model the interaction between the ice rubble, ice sheet and conical pier face, and the flexural failure in the ice sheet. The driving forces and the end moments due to the driving force and contact forces are applied to the support contact points between the ice sheet and the conical face. Finally, the total horizontal load is calculated by summing the horizontal loads due to the ice rubble load on the pier and breaking load for flexural failure of the ice sheet.

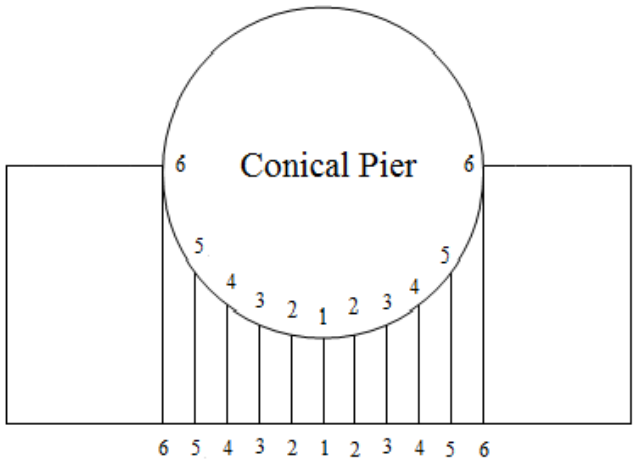

Figure 2. Ice sheet divided into ten horizontal strips with section 1-1 being the middle section (Wong, 2014)

FLEXURAL FAILURE EVENTS

Flexural failure is the predominant ice failure mechanism at the Confederation Bridge. A significant number of limit driving events has also been observed at the Bridge as discussed by Tripathi et al. (2007) and Shrestha et al. (2009). This paper will focus on flexural failure event loads only. The annual maximum flexural loads, based on ice events from 17sec and 15 sec average data, for piers 31 and 32 ranged from 1.29 MN to 6.74 MN and 1.25 MN to 3.6 MN respectively. The annual maximum loads for events failing in flexural are listed in Table 1.

Table 1: Annual maximum flexural loads at either side of both piers, P31 and P32

Year	P31 Load (MN)		P32 Load (MN)	
	NW side	SE side	NW side	SE side
1998	3.8	-3.31	No data	No data
1999	3.5	-3.11	2.77	-1.34
2000	3.45	-1.96	2.33	-1.40
2001	2.26	-1.84	2.12	-1.88
2002	2.42	-2.25	2.26	-1.40
2003	6.74	-2.78	2.27	-2.68
2004	3.09	-1.79	No data	-1.03
2005	3.82	-2.10	3.60	-1.94
2006	1.29	-0.86	1.44	-0.79
2007	3.25	-2.96	2.27	-1.17
2008	6.09	-2.78	No data	No data
2009	3.44	-2.39	2.82	-1.61
2010	1.53	-1.47	1.25	-0.75

Comparison of Measured Load and Model Load

Tibbo (2010) compiled 100 flexural failure events from Confederation Bridge monitoring data and compare the performance of four flexural failure models (Ralston, 1977; Nevel, 1992; Croasdale, 1994; and Mayne, 2007) against full scale trigger load data at pier P31. The

predicted loads from the four flexural failure models against measured loads are shown in Figure 3. In her study she concluded that on average all models both underpredicted and overpredicted the ice loads, with Nevel model predicting the highest load. Based on the scatters around 1:1 slope line, more accurate predictions came from the Mayne model (Tibbo, 2010; Wong et al., 2016).

Wong (2014) used a subset of 10 out of 100 flexural failure events used in Tibbo (2010) study to validate his model. Figure 4 shows the predicted load values from Wong model along with loads from Croasdale and Mayne model. For the selected ten events, Wong model gives better load prediction than the Croasdale and Mayne models. Since the Wong rubble pile model considers three dimensional geometry of rubble pile observed at Confederation Bridge, the rubble pile model is more accurate and realistic.

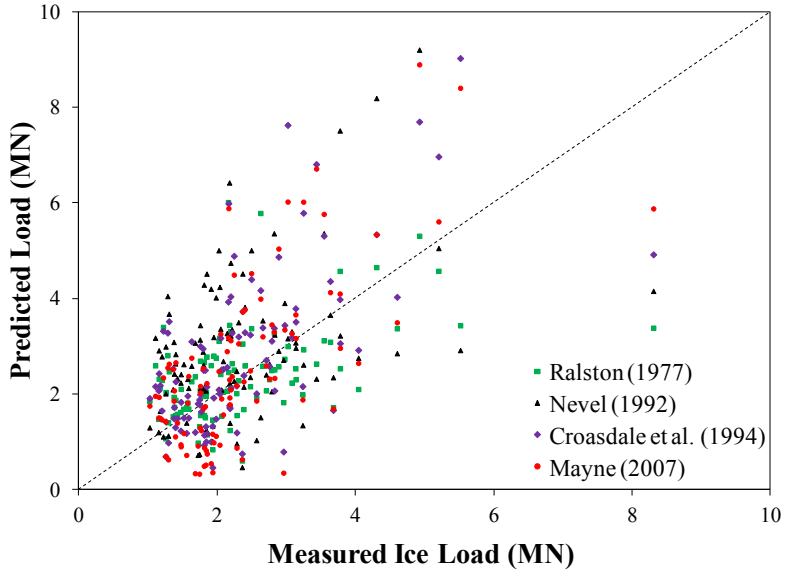

Figure 3. Measured ice load versus predicted ice loads by flexure failure models (modified after Tibbo, 2010)

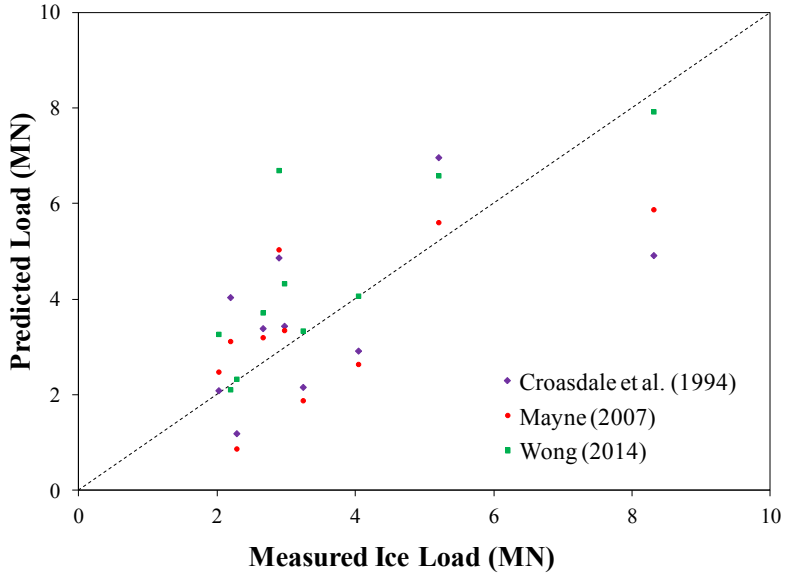

Figure 4. Measured ice load versus predicted ice loads by flexure failure models (modified after Wong, 2014; Wong et al., 2016)

As already discussed, both Mayne model and Wong model were developed based on ice-structure observation at Confederation Bridge and both consider the double conical section and the non-linear rubble pile that is often observed. However, the performance of Wong (2014) model has been validated against only 10 dataset (Wong, 2014; Wong et. al. 2016) and it needs to be expanded for additional full scale data before it could be used for further assessment. Tibbo (2010) flexural failure model assessment suggested Mayne model to be more accurate model for Confederation Bridge data. Hence, for this paper, the model loads for flexural failure events are calculated using Mayne's flexural failure model. The ice interaction data required for the model input is derived from ice video recording. As only daylight data can be extracted from video, the analysis is limited to events occurring during day only. The mechanical parameters such as flexural strength, modulus of elasticity and friction coefficient which are not measurable from video are estimated based on sensitivity analysis (Tibbo, 2010; Shrestha, 2012).

The scatter plot of model load and measured load, both event load and trigger load, are shown in Figure 5 and Figure 6 for piers P31 and P32 respectively. As shown in figures, most of the model loads are within ±1MN of the measured loads. Comparing the model loads with event loads, about 93 % of model loads lies within ±1MN of the measured load. While considering trigger loads, about 71 % of model load for P31 and about 62 % of model load at P32 are within ±1MN of the trigger load. The design load for any structure should never be underpredicted and thus for any model the percentage of underpredicted load are major concern. The model load should be compared with trigger load whenever possible. Considering the trigger loads, about 28% of model loads for P31 and about 38% of model loads for P32 lies outside of lower boundary of 1:1 line and again about 16 % of predicted loads were within ± 10% of trigger loads. In general, when 100% breaking loads is considered, majority of the events loads were overpredicted and the trigger loads were underpredicted. Based on the full scale observation, Mayne incorporated a range of potential failure ice loads: minimum, maximum and average model load. The minimum ice load is sum of the rubble load and 25% of the breaking load and the maximum ice load is sum of the rubble load and 75% of the breaking load. The average load is rubble load plus 50% of the breaking load. Figure 7 and Figure 8 shows the scatter plot of the model load considering 25%, 50% and 75% of breaking load contribution versus measured loads for piers P31 and P32 respectively. The recommended range of model loads (25 % to 75% of breaking load) underpredicted the measured loads especially when comparing it with trigger load, so it is advisable to use 100% of the breaking load for Mayne model.

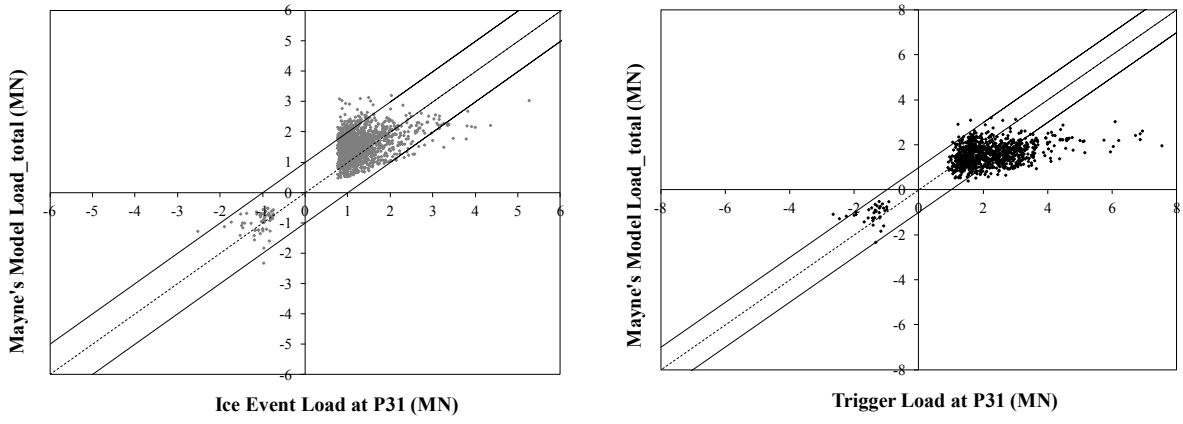

Figure 5. Predicted total load vs. measured ice load: ice events (left) and trigger load (right) at P31 with ±1MN boundary line

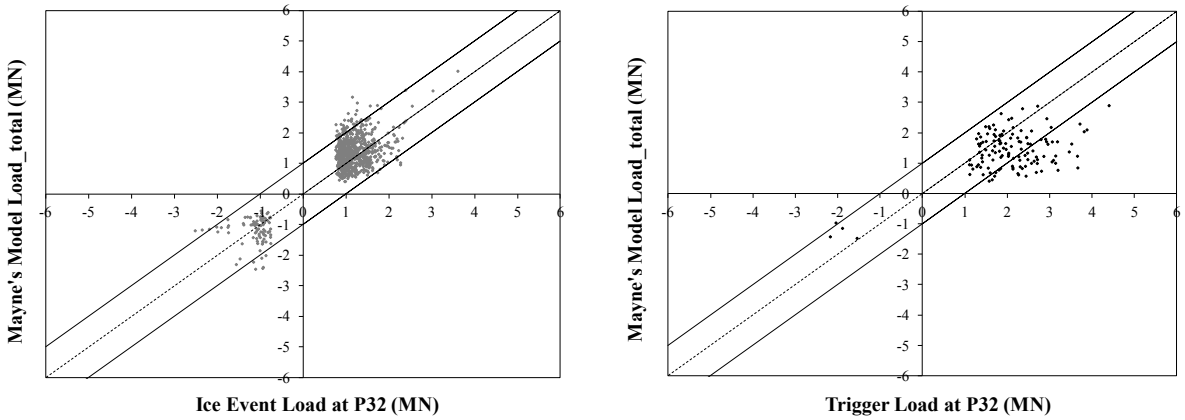

Figure 6. Predicted total load vs. measured ice load: ice events (left) and trigger load (right) at P32 with ±1MN boundary line

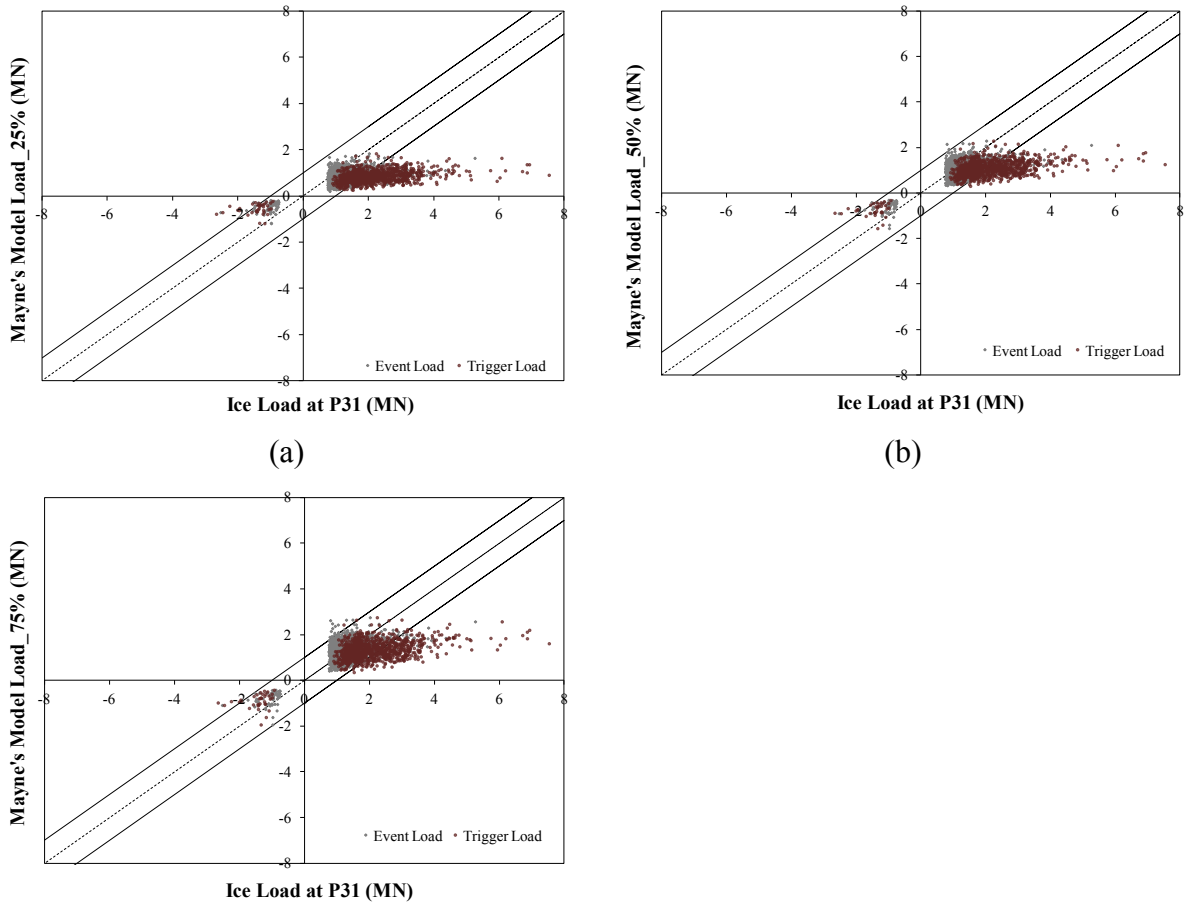

Figure 7. Predicted load: (a) min (25% of breaking load), (b) mean (50% of breaking load), and (c) max (75% of breaking load) vs. measured load, event and trigger, at P31 with ±1MN boundary line

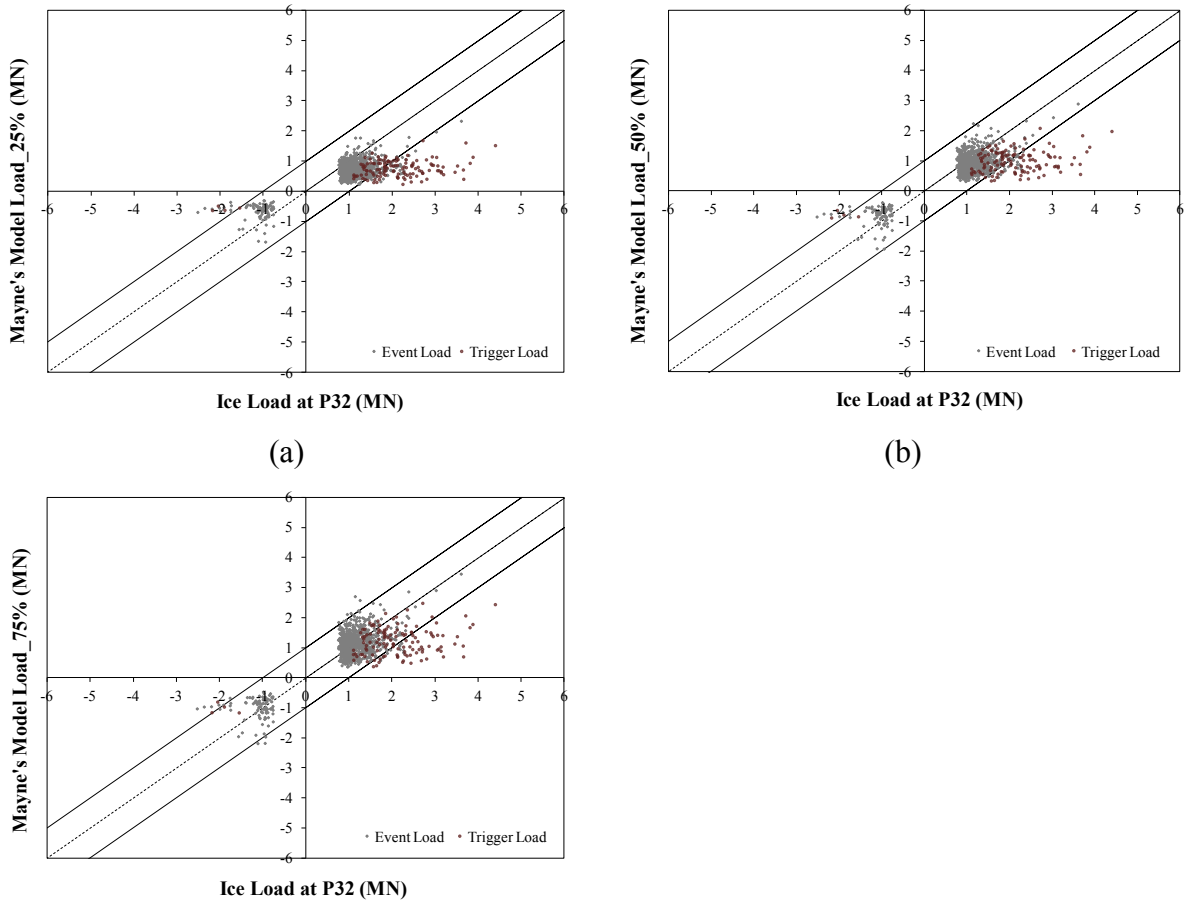

Figure 8. Predicted load: (a) min (25% of breaking load), (b) mean (50% of breaking load), and (c) max (75% of breaking load) vs. measured load, event and trigger, at P32 with ±1MN boundary line

ICE LOAD AND EVENT PARAMETERS

Ice parameters have always been uncertain factors while estimating ice action on the structures. Various studies have been carried out to investigate the relationship between ice geometric parameters and their effects on ice load, individually or combined. However, the conclusions vary between different studies. Conical structures are more effective in reducing the forces associated with interactions with ice features. Still, the failure against the conical structures is a complicated process which involves a number of different parameters affecting ice load on the structure. In this section, three important parameters: ice thickness, ice velocity and rubble pile are analyzed to study their effect on ice load and relation between these parameters.

The event specific parameters for flexural failure events at both piers occurring during daylight hours are extracted from image analysis of the video imagery. These parameters include: ice speed, ice thickness, pileup or ride-up height, rubble angle and upper pile length. The ice thickness is determined from ice pieces within the rubble pile or ride up ice. For each event, multiple ice thickness measurements are taken, if available. To define rubble geometry, pile up height, rubble angle, and upper pile length are measured. The ice sheet velocity is determined from two images taken approximately 10 sec apart and measuring the distance of

a particular landmark on the moving ice sheet. Multiple landmarks on the ice sheet surface are identified in each set of pictures and velocity is averaged for a particular event time.

The measured ice thickness for associated events (i.e, loads ≥0.75 MN) varied from 0.17 to 1.6 m. Ice thickness less than 0.17 m was also observed but was not accounted for in the ice events; hence they are not considered in this study. The average ice velocity ranged from 0.012 to 1.64 m/s. The stall events have been excluded in this analysis.

For the ice events, the rubble pile height measured above mean sea level varied from 0.65 m to 6.21 m at P31 and 1.12 m to 6.67 m at P32. The rubble pile-up height data for pier P31 is normally distributed with a mean of 3.4 m and standard deviation of 0.74 m (Figure 9). Similarly, for pier P32, the rubble pile-up height is normally distributed with a mean value of 3.37 m and standard deviation of 0.76 m (Figure 9). For both piers, around 70 % of pile-up height measurements lie within mean ± 1*standard deviation and 95 % of measurements lies within mean ± 2*standard deviation, as shown in Table 1. Combining the information from both piers, the majority of events had rubble height in range of 2.2 to 4.5 m suggesting pile up occurring between cone 1 i.e., the 52º conical section and cone 2, the 78º conical section. The transition from the lower 52º cone to the upper 78º cone occurs at 2.6m above the mean sea level. The observations showed that the vast majority of rubble piles extend above this transition zone.

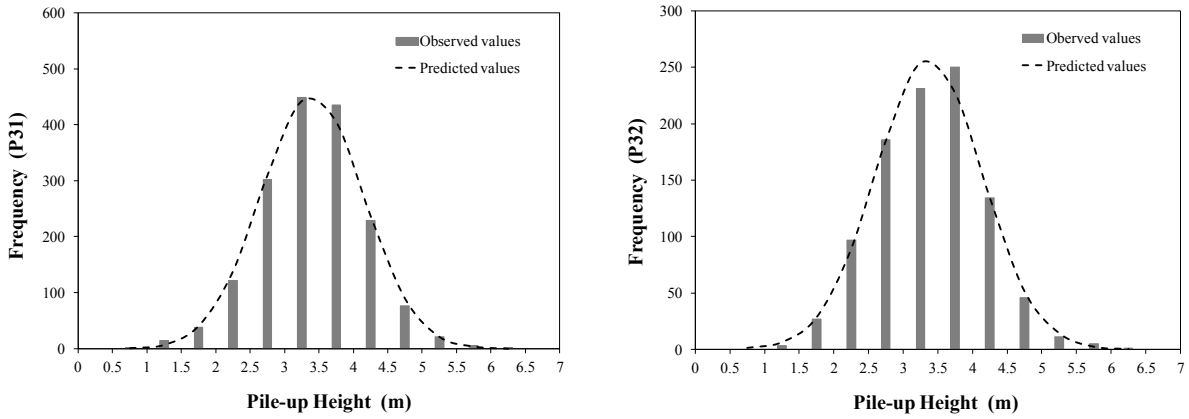

Figure 9. Distribution of pile-up height at P31 (left) and P32 (right)

Table 1. Cumulative distribution of pile-up height measurements

Mean ± X*std dev	P31, Pile-up height		P32, Pile-up height	
	Range	Percentage	Range	Percentage
μ ± 0.5*σ	3.03 – 3.77 m	39.73 %	2.99 – 3.75 m	37.64 %
μ ± 1.0*σ	2.66 – 4.14 m	70.31 %	2.61 – 4.13 m	69.63 %
μ ± 1.5*σ	2.29 – 4.51 m	87.84 %	2.23 – 4.51 m	87.59 %
μ ± 2.0*σ	1.92 – 4.88 m	94.92 %	1.85 – 4.89 m	95.96 %
μ ± 3.0*σ	1.18 – 5.62 m	99.41 %	1.09 – 5.65 m	99.50 %

Effect of Ice Speed on Ice Load

The momentum of the ice is related to the velocity of ice, which affects the load it can impart to a structure during an impact. Brown (2008) study showed a weak relationship between ice

loads and ice velocity. He used the Confederation Bridge data from 1998 to 2000 to examine the relationship. This paper incorporates data from 1998 to 2010 to examine any correlation between ice velocity and ice load. Figure 10 illustrates the scatter plot of the measured average ice load and speed of the interacting ice at piers P31 and P32. The plot represents all data for which the speed was measured, and average ice thicknesses ranging from 0.24 m to 0.96 m. Events with zero velocity, representing events from limited driving forces, have been excluded from the analysis. To study the relationship between measured data two approaches are considered, firstly considering all data and secondly taking only upper bound dataset. Considering all data, the relationship between measured load and ice velocity was weak. While using only the upper bound dataset, the envelope curve shows exponential decrease in load with increasing ice velocity (Figure 10). The upper bound relation for measured loads and ice velocity are represented by equation 1 and 2 for two piers. For pier P32, due to lack of data the event load due to limit stress condition is limited to maximum of 3 MN only, thus the envelope curve is much lower than that of pier P31.

$$F_{avg,P31} = 7.85\mathrm{e}^{-0.99\mathrm{v}} \qquad with\ R^2 = 0.87 \tag{1}$$

$$F_{avg,P32} = 4.29\mathrm{e}^{-0.69\mathrm{v}} \qquad with\ R^2 = 0.88 \tag{2}$$

where, F = ice load (MN) and v = ice velocity (m/s)

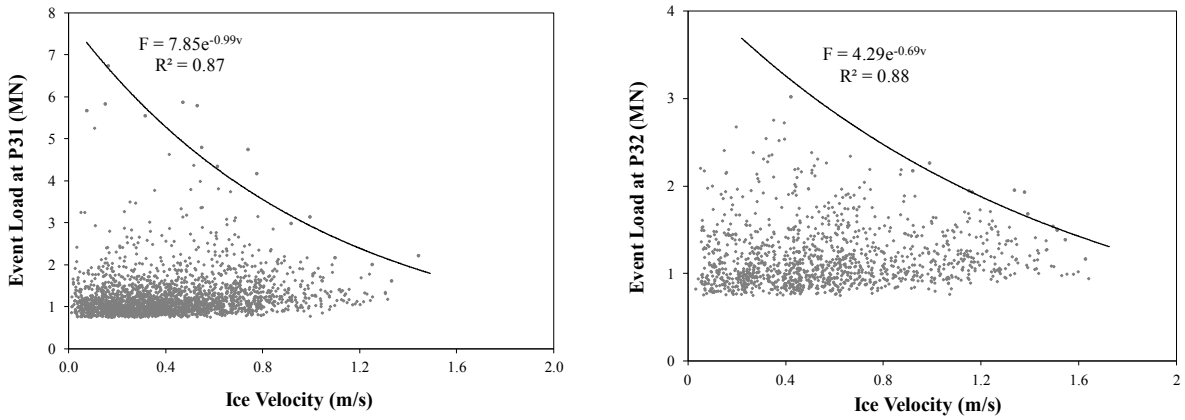

Figure 10. Average ice load against ice velocity at pier P31 (left) and P32 (right)

Effect of Ice Thickness on Ice Load

Ice thickness is one of most important parameters in any flexural failure model. The theoretical flexural failure term depends on the thickness powered by some value (for beam on elastic foundation, the bending term is proportional to the power 1.25); rideup and rubble terms are also related to ice thickness. All flexural failure models (Croasdale, Ralston, Nevel, and Mayne models) reported an increase in load for an increasing ice thickness (Tibbo, 2010). Figure 11 illustrate the plot between the measured average ice load and ice thickness at piers P31 and P32. The stall events have been excluded from the analysis. Taking all data into account, the relationship between measured load and ice thickness is weak. While considering only upper bound dataset, best-fit curve represents a power relationship with increasing ice load for increasing ice thickness (Figure 11). The relationship between measured load and ice thickness is represented by equation 3 and 4 for the two piers. Again due to data limitation the envelope curves for pier P32 is much lower than that of pier P31. As expected the indices in both cases are less than the breaking term index of 1.25, accounting for the effects of the rubble pile.

$$F_{avg,P31} = 6.16\text{h}^{0.95} \qquad with\ R^2 = 0.96 \tag{3}$$

$$F_{avg,P32} = 3.52\text{h}^{0.58} \qquad with\ R^2 = 0.89 \tag{4}$$

where, F = ice load (MN) and h = ice thickness (m)

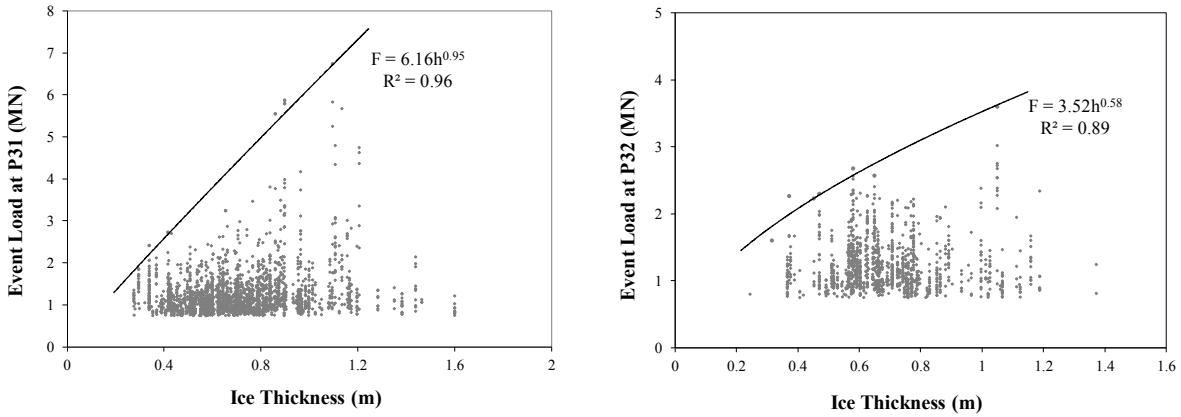

Figure 11. Average ice load against ice thickness at pier P31 (left) and P32 (right)

Effect of Pile-Height on Ice Load

Rubble pile load contribution is the most significant in flexural failure of ice on the conical structures. The shape and size of the rubble pile depend on the surface conditions, ice thickness, ice velocity and piece size (Mayne and Brown, 2000). Figure 12 shows the scatter plots of measured average ice load and rubble pile height at piers P31 and P32 respectively. These plots clearly show that the load increases with increase in rubble pile height. Considering only the maxima, the best-fit trend line suggest power relationship, where equation 5 and 6 represents envelope curve for piers P31 and P32 respectively.

$$F_{avg,P31} = 1.87\text{H}^{0.8} \qquad with\ R^2 = 0.93 \tag{5}$$

$$F_{avg,P32} = 1.15H^{0.65} \qquad with\ R^2 = 0.88 \tag{6}$$

where, F = ice load (MN) and H = rubble pile height (m)

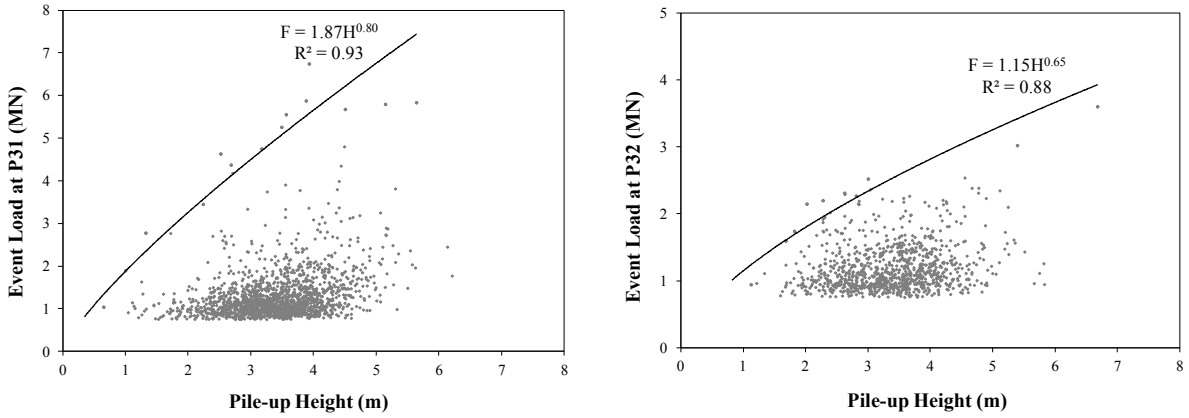

Figure 12. Average ice load against pile-up height at pier P31 (left) and P32 (right)

Relation between Pile-Up Height, Ice Thickness and Ice Velocity

Määttänen and Hoikkanen (1990) and Mayne and Brown (2000) developed relationships to describe the maximum rubble pile height based on ice thickness and ice sheet velocity. The relationships were derived from full scale observations of rubble piles resulting from interaction of level ice with conical structures. Määttänen and Hoikkanen (1990) model is based on field observations made from light piers in the Gulf of Bothnia. The rubble pile is supported by the face of the cone and the advancing ice sheet. Their model considered two cases, (i) when the ice sheet is in contact (supported) with the face of the cone and (ii) when it is not in contact (unsupported) with the face of the cone. The supported or unsupported conditions affect the ability of the ice sheet to support any rubble pile. Using the observations from the Gulf of Bothnia, a relationship is derived between height of rubble pile (H) and ice thickness (h_i) is described by equation 7.

$$H = A.h_i^{0.5} \tag{7}$$

where, the constant (A) is assumed to be 4.5 when rubble pile is unsupported and 6 when the ice sheet is fully supported by the cone.

The Mayne and Brown (2000) envelope curve was based on the full-scale data during period of 1998-2000 at pier P31 from the Confederation Bridge. The relationship between height of rubble pile (H) and ice thickness (h_i) is represented by equation 8. Similarly, the relationship between the height of rubble pile (H) and ice velocity (v) is represented by equation 9.

$$\mathrm{H} = 7.6\mathrm{h_i}^{0.64} \tag{8}$$

$$\mathrm{H} = -3.12\mathrm{v}^2 + 2.07\mathrm{v} + 7.09 \tag{9}$$

Figure 13 shows the plot of the rubble pile height versus ice thickness for piers P31 and P32 using data from 1998 to 2010. Considering only maxima, the envelope curve for the rubble pile height (H) and ice thickness (h_i) is described using a power function, represented by equation 10 and 11 for piers P31 and P32 respectively. Note, once again, the very similar behavior between the rubble piles at the two piers.

$$H_{P31} = 7.52h_i^{0.51} \qquad with\ R^2 = 0.98 \tag{10}$$

$$H_{P32} = 7.50h_i^{0.58} \qquad with\ R^2 = 0.91 \tag{11}$$

The figures also show the upper envelope curve developed by Mayne and Brown (2000) and Määttänen and Hoikkanen (1990). The envelope curve plotted indicates that Määttänen and Hoikkanen model underestimates the height of rubble pile for the ice regime in the Northumberland Strait. The envelope curve with new datasets agrees well with envelope developed by Mayne and Brown (2000). There is an upper limit to the thickness for which this relationship is no longer valid, otherwise the relationship indicates pile heights continue to grow with thickness, however this maximum ice thickness has not been determined.

Figure 14 shows the relation between rubble height and ice velocity at piers P31 and P32. As speed increases, the maximum rubble pile height decreases as a result of improved clearing of the rubble. Considering only maxima, the relationship between decreasing pile height (H) as velocity (v) increases, fitting second order polynomial trend line is represented by equation 12 and 13 for P31 and P32 respectively. The figure also shows the upper envelope curve developed by Mayne and Brown (2000) indicating similar trends.

$$H = -2.97v^2 + 2.0v + 6.54 \qquad with\ R^2 = 1 \tag{12}$$

$$H = -2.77v^2 + 2.26v + 6.56 \qquad with\ R^2 = 0.93 \tag{13}$$

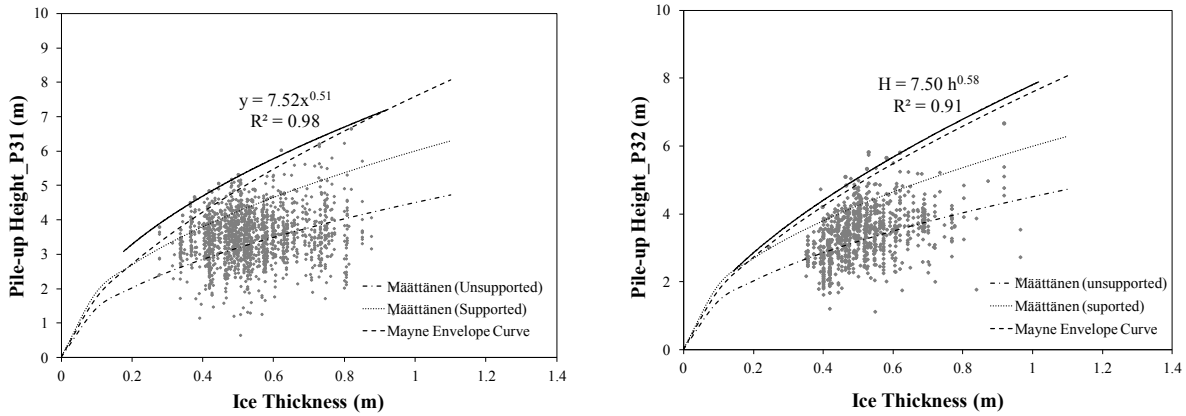

Figure 13. Relationship between rubble pile height vs. ice thickness at pier P31 (left) and P32 (right)

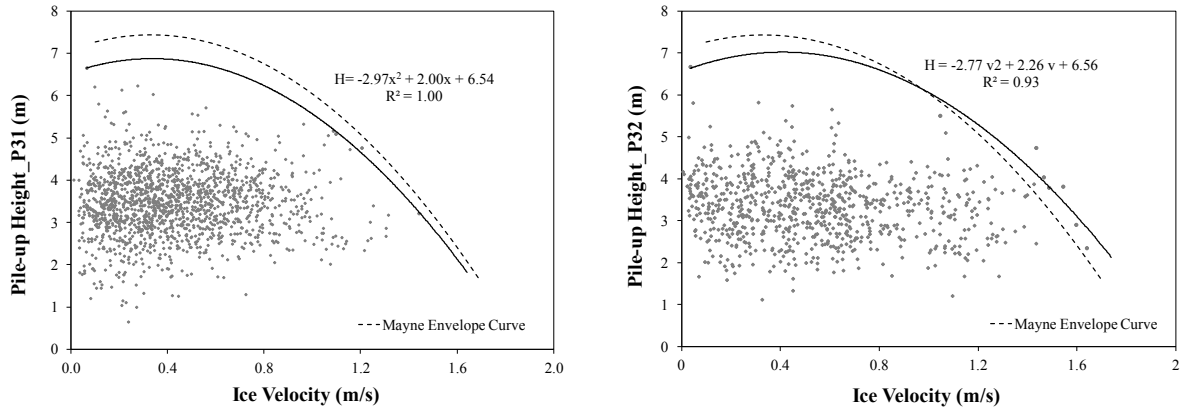

Figure 14. Relationship between rubble pile height vs. ice velocity at pier P31 (left) and P32 (right)

Keel Depth

For the Confederation Bridge, most ridges originate from the Western portion of the Northumberland Strait (Lemeé, 2003). The keel geometric parameters and their effect have been extensively studied for the Confederation Bridge data by Lemée (2003) and Obert (2010). The most recent ridge study for the area have measured maximum keel depths of 7.85 m and 8.49 m for the 2007 and 2008 ice seasons respectively (Obert, 2010). The maximum keel depth recorded between 1996 and 1998 by the Datasonics instrumentation was recorded in 1998 at 15 meters (Brown et. al., 1998). Obert (2010) study has shown that there is no apparent relationship between load and keel depth. Figure 15 shows the plot of load against keel depth and the relationship is very weak. Due to the unique shape of the Bridge pier, no relationship exists between ice load and keel depth as the bottom edge of the ice shield breaks up the keels greater than 4 m, thus reducing the load effect.

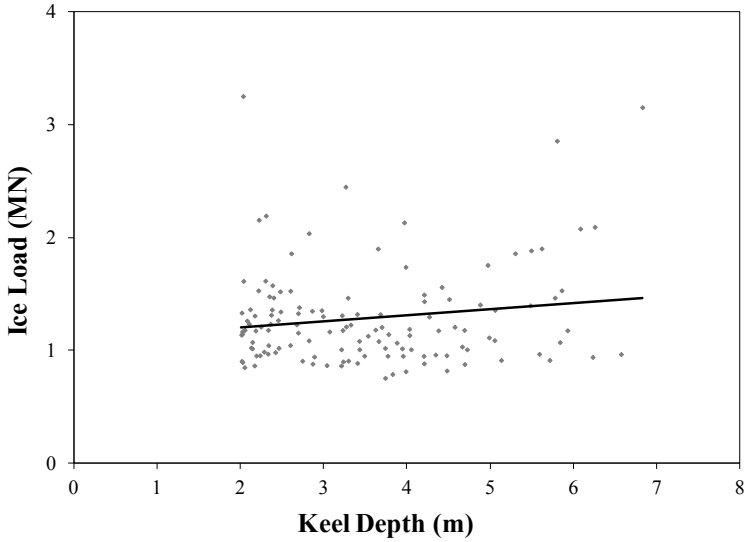

Figure 15. Plot of load against keel depth for P31

PROBABILITY OF EXCEEDANCE

The probability of exceedance plots for the loads for all years from 1998 to 2010 for both piers is shown in Figure 16. The figure indicates that, at the lower levels of probability, negative loads are lower than positive loads for both piers. For pier P32, the curves cross, but this may be an artifact of a limited number of data points. At the 10^{-2} level, the two sets of curves are quite similar with the negative load being about 2.5 MN, and the positive load about 3.0 MN. At higher probabilities of exceedance, the curves from the two piers diverge but, again, this may be a result of few data points. Similarly, Figure 17 shows the probability of exceedance curves for both event and trigger load, irrespective of the loading direction for both piers. Even though the P32 curves are lower than the P31 curves, the probability curves based on event load have a similar pattern but for the trigger load, the curves for the two piers diverge. This is again due to the low number of trigger data at pier P32. For example, at the 10^{-2} level, the event loads are 3.1 MN and 2.8 MN and trigger loads are 4.7 MN and 3.8 MN for piers P31 and P32, respectively.

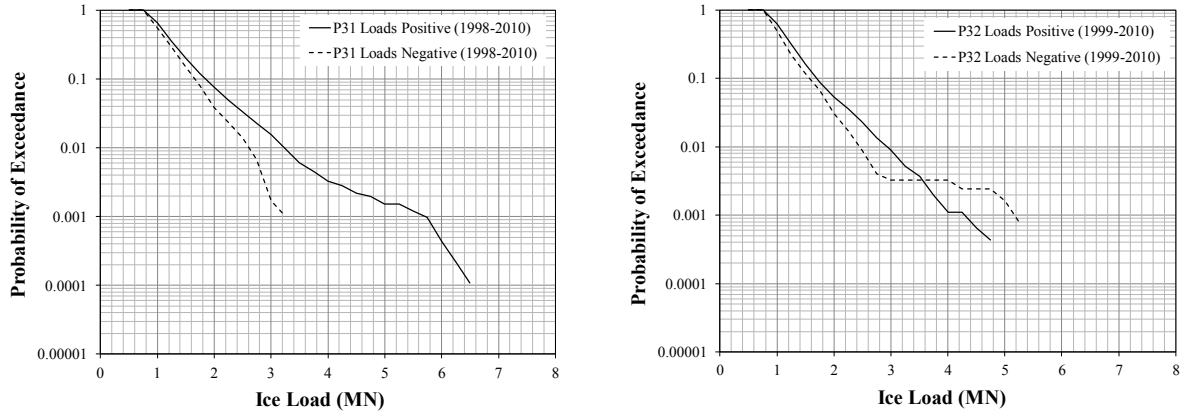

Figure 16. Probability of exceedance curve, P31 (left) and P32 (right)

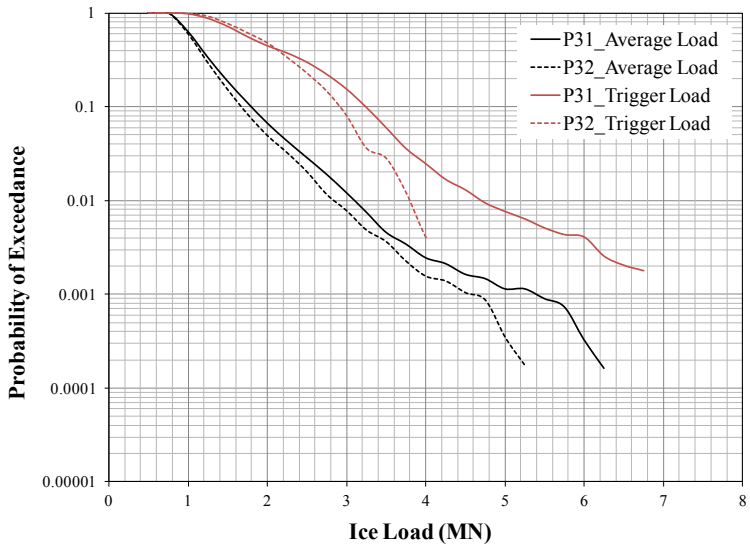

Figure 17. Probability of exceedance curve for average and trigger load for both piers

CONCLUSIONS

This paper presents comprehensive results from the long-term monitoring programme at a Confederation Bridge for both piers P31 and P32. The Mayne's flexural failure model is the most applicable model to assess event based model loads for the Confederation Bridge, as it accounts for both geometries: the double conical section of pier and bilinear rubble profile. The extensive comparison between measured load and model load shows that Mayne's model overpredicted event loads and underpredicted while comparing with trigger loads. About 50% of predicted loads were below 75% of the corresponding trigger load and only about 16 % of loads were within ± 10% of trigger loads. Mayne's model considers 2D rubble pile and use a resolution factor to convert 2D horizontal load into 3D horizontal load. For future study, Wong model should be further investigated to model 3D rubble pile and calculate model loads.

The analysis of the effect of event parameters: ice velocity, ice thickness and rubble height on measured load shows weak correlations between the ice parameters and between load and ice parameters when all events are considered. The weak correlation does not mean they are independent parameters. This suggests that there are many uncertainties involved between ice load and event parameters. A clear relationship exists between event parameters and measured load when only the upper bound data set is considered.

ACKNOWLEDGEMENTS

The authors would like to acknowledge the support of Strait Crossing Bridge Ltd., Public Works and Government Services Canada, the National Science and Engineering Research Council (NSERC) for providing funding. Further, the authors would like to acknowledge the contributions of their colleagues.

REFERENCES

Afanas'ev, D. P., Dolgopolov, Y. V., and Shvaishtein, Z. I., 1971. Ice Pressure on Individual Marine Structures. In Studies in Ice Physics and Ice Engineering, Edited by G.N. Yakovlev, Published by Israel Program for Scientific Translations, Jerusalem, Israel, pp. 50-68.

Bercha, F. G., and Danys, J. V., 1975. Prediction of Ice Forces on Conical Offshore Structures. *Proceeding of 3rd IAHR Ice Symposium*, Hanover, USA, pp. 447-458.

Brown, T. G., Barry, G., Carstens, T., Croasdale, K. R. and Frederking, R., 1994. The Potential Influence of the Prince Edward Island Bridge on the Ice Environment, *IAHR International Symposium on Ice, Trondheim*, Norway, Vol. 2, pp 838-846.

Brown, T., Bruce, J., and Croasdale, K. (1998). *Confederation Bridge Ice Force Monitoring Joint Industry Project Annual Report- 1998*. Calgary: IFN Engineering Ltd.

Brown, T. G., 2007a. Ice Force Monitoring. *Confederation Bridge Engineering Summit*, Charlottetown, PEI: CSCE, pp. 224-254.

Brown, T. G., 2007b. Analysis of Ice Event Loads Derived from Structural Response. *Cold Region Science and Technology,* 47, pp 224-232.

Brown, T., G., 2008. Ice Failure on Conical Structures – Effects of Speed, *Proceeding of the 19th International Symposium on Ice (IAHR)*, 2008, Vancouver, Canada, Vol. II, pp 887-896.

Brown, T. G., Tibbo, S. J., Tripathi, D, Obert, K. and Shrestha, N., 2010. Extreme Ice Load Events on the Confederation Bridge. *Cold Regions Science and Technology*, 60 (2010), pp. 1-14.

Croasdale, K. R., 1980. Ice Forces on Fixed, Rigid Structures. *A State-of-the-Art Report by IAHR Working Group on Ice Forces on Structures*, Edited by T. Carsten, CRREL Special Report 80-26, U.S. Army CRREL, Hanover, N.H., pp. 34-106.

Croasdale, K. R., and Cammaert, A. B., 1994. An Improved Method for the Calculation of Ice Loads on Sloping Structures in First-Year Ice, *Hydrotechnical Construction*, Vol 28, No. 3, pp 174-179.

Edwards, R. Y. and Croasdale, K. R., 1976. Model Experiments to Determine Ice Forces on Conical Structures. *Proceeding of Applied Glaciology Symposium*, Cambridge, U.K., J. of Glaciology, Vol 19, No. 81, pp. 660.

Fredlund, D. G., and Krahn, J., 1976. Comparison of Slope Stability Methods of Analysis. *Canadian Geotech. Journal*, 14(3), pp. 429–439.

Hetényi, M., 1946. Beams on an Elastic Foundation, University of Michigan Studies, *Scientific Series*, Vol. XVI, The University of Michigan Press, Ann Arbor, Michigan, USA.

Lemée, E. M., 2003. *Pressure Ridge Interaction with the Confederation Bridge Piers*. MSc. Thesis, Department of Civil Engineering, University of Calgary, Calgary, Alberta, Canada

Lau, M., 1999. *Ice Forces on A Faceted Cone due to the Passage of a Level Ice Field*. PhD Thesis, Memorial University of Newfoundland, St. John's, NF.

Lavoie, N. Y., 1966. *Ice Effects on Structures in the Northumberland Strait Crossing. In Ice Pressures against Structures*, NRC Technical Memo No. 92 (NRC No. 985), Ottawa.

Määttänen, M., and Hoikkanen, J., 1990. The Effects of Ice Pile Up on the Ice Force of a Conical Structure, *Proceeding 10th International Symposium on Ice*, Vol. II, Espoo, Finland, pp 1010-1021

Mayne, D. C., and Brown, T. G., 2000. Rubble Pile Observations, *Proceeding 10th International Offshore and Polar Engineering Conference*, Seattle, USA, pp 596-599.

Mayne, D. C., 2007. *Level Ice and Rubble Actions on Offshore Conical and Sloping Structures*. PhD. Dissertation, Department of Civil Engineering, University of Calgary,

Canada.

Nevel, D., 1992. Ice Forces on Cone from Floes, *Proceeding IAHR Symposium on Ice 1992*, Vol. 3, Banff Canada, 1391-1404.

Obert, K. M., 2010. *Ridge Keel Geometry and Interaction with the Confederation Bridge*. MSc. Thesis, Department of Civil Engineering, University of Calgary, Calgary, Alberta, Canada.

Pearce, J. C., and Strickland, G. E., 1979. Ice Forces on Conical Structures. *Proceeding of 11th Offshore Technology Conference*, Vol. 4, Paper No. 3635, Houston, USA, pp. 2407-2414.

Ralston, T., 1977. Ice Force Design Considerations for Conical Offshore Structures, *Proceeding of International Conference on Port and Ocean Engineering Under Arctic Conditions (POAC)*, Vol. II, Memorial University of Newfoundland, St. John's Newfoundland, Canada, pp 741-752.

Shrestha, N., Tripathi, D., Mayne, D., and Brown, T. G., 2009. Analysis of Limit Driving Force Events on the Confederation Bridge. *Proceedings of the 20th International Conference on Port and Ocean Engineering under Arctic Conditions (POAC09)*, Luleå, Sweden.

Shrestha, N., 2012. *Ice Action Database for the Confederation Bridge Piers*. PhD. Dissertation, Department of Civil Engineering, University of Calgary, Calgary AB, Canada, 2012.

Tibbo, J.S., 2010. *Flexural Failure of Sea Ice*. MSc. Thesis, Department of Civil Engineering, University of Calgary, Calgary, Alberta, Canada.

Tripathi, D., Shrestha, N., and Brown, T. G., 2008. February 13, 2007 Limit Driving Force Event on the Confederation Bridge. *8th International Conference and Exhibition on Performance of Ships and Structures in Ice (ICETECH),* Banff, AB, pp. 238–242.

Wong, C.K., 2014. *Development of a Three-Dimensional Model for Ice Rubble Interactions on Conical Structures*. M.Sc. Thesis, Department of Civil Engineering, University of Calgary, Calgary, AB, Canada.

Wong, C.K., Brown, T.G., and Robertson, J.S., 2016. Assessment of Flexure Failure Models Using Loads Measured on the Conical Piers of the Confederation Bridge During 1998–2008. *Journal of Offshore Mechanics and Arctic Engineering*, Vol. 139/Issue 1, DOI: 10.1115/1.4034527.